Experimental and theoretical model of a concentrating photovoltaic and thermal system

C. Renno* and F. Petito
Department of Industrial Engineering, University of Salerno,
Via Giovanni Paolo II, 132, 84084 Fisciano (Salerno), Italy.

Abstract

The experimental and theoretical analysis of a concentrating photovoltaic and thermal system (CPV/T) presented in this paper allows to evaluate the electrical parameters of the system, the concentration factor, the cell temperature in different working conditions and the fluid temperature. In particular, the experimental values of the cell temperature represent the input of a model developed in ANSYS-CFX. This model evaluates the theoretical temperature values of the fluid that flows into the cooling circuit of the CPV/T system, designed with the CATIA software. Hence, both electrical and thermal parameters have been analyzed in order to evaluate the potential energy production of a concentrating photovoltaic and thermal system. Different configurations of the CPV/T system have been analyzed and the value of the concentration factor has been determined by means of an experimental procedure. The experimental and theoretical electric powers are compared in different climatic conditions considering a solar radiation included between 500 and 900 W/m^2. The electric efficiency is also evaluated as function of solar irradiance and cloudiness. Moreover, the fluid temperature as function of the experimental cell temperature is determined in different working conditions by means of the ANSYS model. The fluid temperature is also theoretically determined varying the operating conditions along the circuit. Finally, a study of the electrical and thermal performances represents a key-factor to develop a more complex prototype of a CPV/T system.

Key-words: concentrating photovoltaic and thermal system, experimental analysis, ANSYS model, heat recovery.

1. Introduction

In a concentrating photovoltaic system (CPV) the sunlight is concentrated on triple-junction solar cells by means of an optical device and higher temperatures are also obtained [1]. This has an impact on the electric performances and, differently from the traditional photovoltaic systems, on the possible recovery of thermal energy at high temperature. Hence, the concentrating photovoltaic and thermal systems (CPV/T) allow to obtain electric and thermal energy [2]. Therefore, the heat removal becomes a strategic factor that affects the CPV/T system configuration [3]. Many applications are investigated in literature in order to evaluate the potential of the CPV/T systems. In [4] a review of various cooling technologies available for CPV systems is presented. The technology should be reliable and maintain a low and uniform cell temperature. In [5] the fluid which cools the cells is accumulated in a tank. In [6] a concentrating dish is linked to a system of tubes evacuated to have an efficient thermal energy production. In [7] the performances of a CPV/T system with a Fresnel concentrator are studied. In [8] a new multi-layer manifold micro-channel cooling system for concentrating photovoltaic cells is presented. In [9] a CPV/T system is designed in order to recovery thermal energy and to increase the electric production. In [10] a compound parabolic concentrator is modified to evaluate the performances of a new solar concentrator working simultaneously as electricity generator and thermal collector. In [11] related to the electric, heating and cooling loads of a domestic user, the design and model of a CPV/T system are studied. In [12] the optimized value of the concentration factor able to provide a fluid outlet temperature that satisfies the thermal and cooling demands and to decrease the CPV/T system size, is obtained in each working condition. Hence, there are several CPV/T systems that allow a combined energy production, but it is not possible to obtain a standard configuration [13]. Therefore, it is important to evaluate accurately for each operating condition both the electrical and thermal performances of a CPV/T system. In particular, it is necessary to evaluate the cell temperature that depends on the concentration of the solar radiation, and influences the electrical performances of the same cell. This is basic to evaluate the temperatures reached by the working fluid in a CPV/T system. These evaluations can be carried out both experimentally and theoretically. In [14] a numerical and experimental study of a U-shaped solar energy collector model of a CPV/T system is presented in order to evaluate the maximal thermal and electrical power related to an optimum volumetric flow rate. The simulation of a high concentrating photovoltaic module by means of neuronal networks, adopting the direct normal irradiance spectrally corrected and the cell temperature, is presented in [15]. The model of a linear concentrating photovoltaic system with an active cooling system, is reported in [16]. In [17] the dynamic model of a CPV/T system is theoretically determined by means of the finite element method. In [18] a three dimensional heat transfer model is presented for a design of new concentrating photovoltaic system. So, it can be noted that the thermal recovery depends on the evaluation of the cell temperature whose value cannot easily determined theoretically in each operating condition [19]. The cell temperature, which affects the heat recovery, is strongly linked to the concentration factor [20]; these factors influence several cell parameters such as the photo-generated current [21]. Hence, in this paper a specific configuration of a CPV system is presented and studied. The configuration adopted considers the coupling of a Fresnel lens with a triple-junction solar cell and a kaleidoscope as secondary optics. This kind of system has been only partially treated in literature. In particular, the innovative aspect of the analysis reported in this paper is related to the secondary optics use in order to achieve a high concentration factor. Moreover, the system designed is experimentally analyzed from an electrical and thermal point of view, and the cell electrical performances and its temperature are experimentally determined. Different tests are conducted in order to define the concentration factor reached by the designed CPV scheme in standard conditions. Subsequently, by means of a finite element model built in

ANSYS [22] which has as input the experimental cell temperature, the refrigerant fluid temperature is theoretically determined corresponding to different solar radiation and outdoor temperature values. This study analyses the possibility to use a refrigerant fluid, such as a glycol-water solution, for an active cooling of the solar cell in order to obtain also thermal energy. Hence, the ANSYS model allows to evaluate the thermal energy production of a CPV/T system, once experimentally evaluated the cell temperature. Finally, the system electrical performances are also experimentally evaluated taking into account different working conditions.

2. Theoretical model

In order to evaluate accurately the electrical and thermal performances of a CPV/T system, in this paper the cell electric power and its temperature are experimentally determined. In particular, by means of a model built in ANSYS [22], which has as input the cell temperature values experimentally obtained, the cooling fluid temperature is determined corresponding to different working conditions. Photo and scheme of the experimental plant are respectively reported in the Figures 1 and 2. In Figure 3 the flow-chart of the experimental-theoretical analysis is reported. This study of the electrical and thermal performances represents a key-factor in order to develop a more complex prototype of a CPV/T system. The experimental analysis has been realized following three phases. The first step has been the electrical characterization of the system in the standard conditions and the C evaluation. The second phase analyzes the electrical performances of the CPV system in terms of electric power and efficiency in different conditions. The third step matches the experimental tests with the theoretical analysis developed in ANSYS-CFX. In particular, the experimental values of the cell temperature represent the input of the thermal model which evaluates the cooling fluid temperature of the CPV/T system considered in this paper. The cooling circuit for the ANSYS thermal simulations has been designed with the CATIA software. Hence, both electrical and thermal aspects are analyzed in order to evaluate the energy potential of a CPV/T system.

2.1 Electric model

The CPV/T system electrical power, generally, depends on different external and internal parameters. External variables such as installation site, direct solar irradiance and atmospheric conditions represent not controllable external conditions. Internal parameters are the concentration factor (C), the cell temperature (T_c) and the efficiency (η_c). Another important parameter is represented by the number of cells, especially when a CPV/T module is analyzed. The model general assumptions adopted are: steady state and radiation uniformly concentrated along multi-junction cells. By means of the experimental system before described, the instant direct irradiance (G) is available for each time step. Hence, the direct solar irradiance which reaches the MJ cell can be evaluated as in [23]:

$$G_{inc,c} = G_{dir} \cdot C \cdot A_c \cdot \eta_{opt} \quad (1)$$

where the incident direct irradiance ($G_{inc,c}$) on the solar cell depends on the C value and the cell area (A_c), previously defined. The optical efficiency (η_{opt}) has been considered constant and equal to 0.88 considering the Fresnel lens adopted [24]. Hence, the theoretical electric power can be expressed as:

$$P_{th,c} = G_{inc,c} \cdot \eta_{c.th} \quad (2)$$

The cell theoretical efficiency ($\eta_{c,th}$) is influenced by the cell operating temperature and it can be expressed by means of the manufacturer instructions as:

$$\eta_{c,th} - \eta_{ref} = \sigma_t \cdot (T_c - T_{ref}) \quad (3)$$

where T_{ref} is the reference temperature equal to 25°C and η_{ref} is the reference efficiency corresponding to the concentration value, according to the cell manufacturer indications reported in Table 1. The temperature coefficient σ_t indicates the efficiency percentage reduction as function of the temperature increase, its value has been set at -0.04%/°C in a range 10°C/100°C [25]. T_c corresponds to the experimental values measured. Hence, considering a module composed by a variable cells number, the CPV/T system electric power can be estimated as:

$$P_{th,CPV/T} = P_{th,c} \cdot N_c \cdot \eta_{mod} \quad (4)$$

where the module efficiency (η_{mod}) until 100 cells is equal to 0.95 [13], and N_c represents the cells number which constitute the module. The theoretical electric power of the CPV/T system can be compared with the real electric power observed by means of the experimental system. The cell power can be evaluated for each time step as:

$$P_c = V \cdot I \quad (5)$$

where V and I are respectively the cell voltage and current measured by means of a data logger. As indicated in Figure 2, the cell has been connected to a variable load in order to achieve the maximum power at each time. The ideal electrical output power is defined as the product between the open circuit voltage (V_{OC}) and the short circuit current (I_{SC}); hence, the fill factor (FF) which represents the ratio between the real and the maximum electric power is equal to [21]:

$$FF = \frac{P_c}{V_{OC} \cdot I_{SC}} \quad (6)$$

The effective cell efficiency can be evaluated as:

$$\eta_c = \frac{P_c}{G_{inc,c}} \quad (7)$$

where the direct solar irradiance $G_{inc,c}$ has been defined in the Equation 1; it represents the total power that reaches the triple junction solar cell and theoretically convertible into electricity. The real cell efficiency can be compared with the theoretical value calculated in order to analyze how the experimental system presented in this paper deviates from the best operating conditions.

2.2 Thermal model

The energy balance for the tube and thermal fluid is represented by means of the equations:

$$m_t c_t \, {\partial T_t}/{\partial \theta} = A_t K_t \, {\partial^2 T_t}/{\partial x^2} + \alpha A_t G - \pi d_o \bar{h}_a (T_t - T_a) - \pi d_i \bar{h}_i (T_t - T_f) \quad (8)$$

$$m_f c_f \, {\partial T_f}/{\partial \theta} + \dot{m}_f c_f \, {\partial T_f}/{\partial x} = \pi d_i \bar{h}_f (T_t - T_f) \quad (9)$$

where α is the absorptivity coefficient [26] of the solar cell, T_t and T_f are respectively the tube and fluid temperatures. The CPV/T system model allows also the calculation of the fluid outlet temperature, generally water and glycol, used to cool the cells and to provide the thermal energy [27]. The solar radiation focused on the triple-junction cell determines the heating of the tube, placed immediately below the cells, and then of the fluid. The insulating with aerogel is used to avoid heat loss (Figure 4a). Once known the dimensions and conductivities of the cell, tube, epoxy resin and insulating, the thermal resistances values and then the global conductance value can be determined (Figure 4b). Hence, determining experimentally the cell temperature and adopting the ANSYS model, it is possible to evaluate the fluid temperature along the tube.

2.3 Numerical solution

The main aim of CPV/T system thermal analysis is the fluid temperature evaluation that flows in the tube. The thermal model described in Section 2.2 has been simulated using the Computational Fluid Dynamics (CFD) techniques. In particular, the ANSYS CFX [21] software has been employed in order to evaluate the refrigerant fluid temperature in different working conditions. First of all a geometric model of the cooling circuit with the solar cells has been realized with the CATIA software [28], as shown in Figure 5. In the last years the virtual prototyping techniques, and so the CAD modeling (CATIA, SolidWorks, NX, Creo) and multiphysics software (ANSYS, COMSOL), are becoming very important for the design and development of the engineering systems [29-30]. In the computational phase the proper surfaces during the domain definition have been selected. An appropriate meshing selection has been then defined to solve the numerical model [31]. The generated mesh presents tetrahedral elements, with a higher density in the zones where the heat transfer is more interesting. In order to evaluate T_f, three computational domains have been defined. Cells and channels are indicated as solid domain, while the cooling fluid is a fluid domain. The heat transfer phenomenon in the different working conditions, insulated zone and not insulated zone (Figure 4b), has been evaluated using the proper boundary conditions on the heat exchange surfaces in the CFX software. The domains definition can be observed in Figure 6: in blue the fluid domain, in yellow the tube domain and in red the cell domain. The cells have been fixed to the tubes with an epoxy resin thickness equal to10^{-4} m, while the copper tube thickness is $3{\cdot}10^{-3}$ m. The insulated zone presents an insulating in aerogel with a conductivity of 0.014 W/mK and a thickness of $5{\cdot}10^{-3}$ m. The thermal resistance model (Figure 4b) allows to define in the numerical model the conductive and convective heat transfer coefficients. In particular, a convective heat transfer coefficient value equal to 6.45 W/m^2 K has been considered referring to the thermal exchange with outdoor air. The domains definitions, shown in Figure 6, allow to simplify the thermal resistances model; the heat exchange surfaces are reduced to three in the computational model of the not insulated zone. Hence, considering the calculated thermal resistances, different values of equivalent resistances are used as boundary conditions. The first takes into account the convective heat exchange coefficient between air and cells. The second considers the series resistance between cell, epoxy resin and copper; the third imposes the convective heat exchange condition between the copper channel and fluid. As for the insulated zone, the domains considered are two: the solid which refers to the copper channels and the fluid which considers the cooling fluid. Hence, only two boundary conditions are introduced into the numerical model taking into account the calculated thermal resistances (Table 2). A fluid velocity of 0.38 m/s, a temperature of 12°C at the inlet section and the atmospheric pressure at the outlet section have been considered in the model. An outdoor temperature included between 10 and 35°C and a solar radiation between 500 W/m^2 and 900 W/m^2 have been considered in the analysis. In order to obtain the temperature field solution, different criterions of convergence have been used: 10^{-4} for the continuity and momentum equations, and 10^{-5} for the energy equation. The computational model is set to simulate the total time period where the sunlight is present, in order to observe the fluid temperature trend in several hours; the time step used is 1s.

3. Experimental analysis

3.1 Experimental plant description

The experimental system presented in this paper, as shown in the Figures 1 and 2, is based on a point-focus configuration that adopts a Fresnel lens as primary optics; a kaleidoscope is adopted as secondary optics. A triple-junction solar cell (InGaP/InGaAs/Ge), placed in the lens focus, and a tracking system complete the experimental plant. The tracking system allows to keep the sunrays perpendicular to the system optics during the day. The Fresnel lens has a diameter of 32 mm. The secondary optics allows to uniform the solar radiation on the cell area avoiding chromatic aberration problems and improving the optics efficiency [32]. The cell used is 5.5x5.5 mm^2 [25] and its characteristics are reported in Table 1 at an environmental temperature of 25°C and a solar irradiance of 100 W/cm^2 (1000 suns). Three thermo-resistances are adopted and respectively placed: below the cell, to evaluate its temperature, on the cell plane and another to measure the outdoor temperature. The experimental data are collected by a data logger that presents five independent analogue channels and eight digital channels bidirectional [33]. The data logger can measure voltage, current, resistance and frequency, and other physical variables may be derived. Hence, the data logger allows to measure the three temperatures above mentioned, the direct solar irradiance and the cell voltage. The CPV system designed has been experimentally realized without the cooling circuit. A "grey model" of the CPV/T system cooling circuit has been developed. In particular, in the thermal model realized in ANSYS, it has been necessary to experimentally determine the input values of the cell temperature [34]. Hence, it is basic an experimental characterization in terms of concentration factor and cell temperature, whose values have been adopted in the thermal theoretical model in order to evaluate the refrigerant fluid temperature. The theoretical thermal model reported in this paper is necessary before to design and realize an experimental thermal recovery system of a CPV/T system. This experimental system could be obtained arranging the cells in series on a tube where the cooling fluid (water-glycol solution) flows; so, more rows can be realized in parallel in order to constitute a CPV/T module. Hence, the concentrated sunlight can be converted simultaneously into electrical and thermal energy.

3.2 Concentration factor evaluation

The concentration factor allows to modify the solar radiant power for area unit by means of optical devices. The experimental system showed in this paper adopts a Fresnel lens in order to amplify the solar irradiance incident on the triple-junction solar cell. Although the concentration factor is theoretically evaluable as ratio between the primary concentrator area and cell area, in this paper it has been evaluated by means of an experimental procedure which takes into account three configurations. The first is only represented by the multi-junction (MJ) cell, the second considers the MJ cell and the kaleidoscope as primary optics. The third is constituted by the experimental CPV system presented in this paper, with Fresnel lens as primary optics and the Kaleidoscope as secondary one. The first configuration presents a concentration factor equal to one, while the second and the third are initially characterized by an unknown C value. C has been experimentally evaluated comparing the short-circuit current (I_{SC}) of the three configurations. Hence, the concentration ratio is evaluated dividing for the configurations considered the short-circuit current (I_{SC}) under concentrated light with the I_{SC} under a unitary C value [35]. So, the concentration ratio of the Kaleidoscope is equal to:

$$C_{Kal} = \frac{I_{SC,Kal}}{I_{SC}} \quad (10)$$

The tests conducted with the same value of solar irradiance equal to 870 W/m^2, have allowed to calculate an experimental value of C_{Kal} equal to about 6.54. Similarly, the value reached in the third configuration, which represents the concentration factor of the whole system (C_{tot}), can be expressed as:

$$C_{tot} = \frac{I_{SC,tot}}{I_{SC}} \quad (11)$$

Referring to the same irradiance conditions of the last case, the C_{tot} value obtained has been 208.6. It is possible to note that an intermediate value of C can be evaluated as the ratio between the short-circuit current under illumination in the third and second configuration:

$$C_{int} = \frac{I_{SC,tot}}{I_{SC,Kal}} \quad (12)$$

The intermediate C value is equal to 31.9. Hence, it allows to validate the C value obtained for the whole system, because all the tests have been conducted in the same conditions and they have demonstrated that:

$$C_{tot} = C_{Kal} \cdot C_{int} = 208.6 \quad (13)$$

This allows an experimental evaluation of C taking into account all possible optic losses. The C value experimentally determined has been employed for the evaluation of the electrical and thermal performances of the system.

4. Results

The experimental plant presented in this paper allows to evaluate the electric energy provided by the concentrating photovoltaic system, and then to study the thermal potential of a more complex CPV/T system whose cooling circuit has been designed with the

CATIA software. The experimental tests have allowed to define both the electrical parameters of the plant presented and the concentration factor. Moreover, the experimental evaluation of the cell temperature in different working conditions represents the input of a model, developed in ANSYS-CFX, able to evaluate the fluid temperature in the cooling circuit, where the solar cells are placed. Hence, both electrical and thermal aspects of a concentrating system have been investigated in this paper.

4.1 Experimental tests

The experimental tests have been realized at University of Salerno between December 2014 and December 2015. The duration of the tests has been of about seven hours a day with a sampling interval of fifteen seconds. First of all an experimental analysis has allowed to define the best configuration of the CPV system changing the optics system. The solution with only the Fresnel lens as optics to focus the sunlight on the receiver, has not been considered because of the chromatic aberration problems. Hence, a kaleidoscope has been employed that has allowed to uniform the solar irradiance on the cell and to reduce also the losses due to the sun tracking. Different configurations have been experimentally evaluated comparing the CPV system behavior with the case of the unitary concentration factor. In particular, the adopted configurations have considered a first case with the kaleidoscope as primary optics, and a second case with the Fresnel lens as primary optics and the Kaleidoscope as secondary one. Fixing the solar direct irradiance, the I_{SC} and V_{OC} values have been obtained together with the maximum power point corresponding to the defined concentration. Moreover, other experimental tests have been realized to evaluate the electric power, electric efficiency and cell temperature in several meteorological conditions: season, direct irradiance intensity and cloudiness. The results experimentally obtained have been compared with the theoretical ones and they represent the starting point for the thermal behavior evaluation.

4.2 Electrical and thermal analysis

The electrical characterization of the experimental plant represents the key-point for the system performance evaluation. The I_{SC} and the V_{OC} values of the MJ solar cell have been evaluated for different configurations. The first case considers only a kaleidoscope as primary optics; the second solution analyzes the whole system configuration with Fresnel lens and kaleidoscope respectively as primary and secondary optics. The values observed for the whole system have been: I_{SC} =0.995 A and V_{OC} = 3.05V. In the maximum power point, the current and voltage values have been: I_{MPP} = 0.759 A and V_{MPP} = 2.45V with an electric power of about 1.862 W. The values observed in the configuration which considers only the kaleidoscope have been: I_{SC}=0.0312 A and V_{OC} = 2.62 V. In the same conditions, the MJ solar cell has presented a short-circuit current of 0.00477A and a open circuit voltage of 2.58 V. Hence, different experimental values of the concentrating factor, have been experimentally evaluated comparing the I_{SC} value of the MJ cell unlighted, with the other two values obtained. The first adopts only the kaleidoscope, the second considers the whole system with Fresnel lens and kaleidoscope. The values measured for the first and second solution are respectively 6.54 and 208.6. This has allowed to evaluate an intermediate C value of 31.9, as shown in Figure 7, which represents the illumination increase of the second solution that considers the whole system. In Figure 7, the MJ cell V-I characteristic under different concentration levels is reported. It can be noted as the V_{OC} increases with the concentration. The whole system configuration has been adopted in the electrical analysis; the C value reached has constituted the empirical value used in the theoretical comparison in terms of electric power and efficiency. In Figure 8 the experimental and theoretical electric powers have been compared taking into account a summer day. The experimental test has been conducted on 23rd June 2015 considering seven hours from 10:30 am to 17:30 pm. Considering a sunny day with an average solar irradiance of 920 W/m^2, the mean experimental power is resulted equal to 1.72 W, while the corresponding theoretical value has been about 2.27 W. The theoretical electric power has been evaluated by means of the Equations 5, 6 and 7 adopting the experimental value of the cell temperature for the efficiency theoretical evaluation. The mismatch of 24% between the theoretical and experimental values could depend on a non perfect tracking or lower real efficiency values. In Figure 9 the same analysis has been conducted for a winter day. The reference experimental test has been realized on 27 January 2015 from 9:30 am to 16:30 pm corresponding to an average solar irradiance of 723 W/m^2. The mean real electric power has been 1.36 W, while the theoretical value has been about 1.95 W. The deviation of 30% is due to the lower cell temperature values that determine a higher theoretical cell efficiency, or to variable meteorological conditions. The comparison between the theoretical and experimental values of the electric power and efficiency, has been very useful. It has allowed to understand that the real electric power is much more influenced by the cell temperature values of what was expected. This means that the cell overheats more of what was expected, and this affects the electric efficiency. Moreover, the theoretical electric model does not consider a loss factor for tracker misalignments, which can occur especially when the solar direct radiation quickly varies. In order to underline this aspect, in Figure 10 the cell electric efficiency has been evaluated in different climatic conditions. In particular, the cell efficiency both for a sunny and a cloudy day is presented together with the related values of solar irradiance. In particular, the values of the daily average efficiency equal respectively to 0.289 and 0.232 have been estimated both for a sunny and a cloudy day. Considering a CPV/T system module with 60 cells, similar to the solar cell experimentally analyzed, the daily electric energy production reaches a value of 686 Wh in a sunny day and 541 Wh in a cloudy day taking into account a module efficiency of 0.95. This value is only referred to the series connection of the 60 cells. Hence, considering the cell efficiency, the overall module efficiency is lower than 30 %. As above said, the results of the experimental analysis allow to evaluate the thermal potential of a CPV/T system. Considering a module with 60 cells, the concentration factor experimentally estimated equal to 208.6 and the circuit shown in Figure 5, the cell temperatures, experimentally evaluated and reported in Figure 11 for different months of the year, represent the starting point for the computational analysis and then the values fixed for the cells in the CPV/T module. Hence, in Figure 12, the fluid temperature trend has been reported considering the cell temperatures values reached in a summer day; corresponding to an average cell temperature of 63°C, the fluid reaches a temperature of about 55°C in four hours. In Figure 13, the fluid temperature has been observed for a winter day. In particular, considering an average cell temperature of 50°C, the fluid temperature after 220 minutes is about 42°C. The fluid temperature, obtained by means of ANSYS-CFX, is reported in Figure 14 corresponding to a low concentration factor. Hence, considering higher concentrating factors and variable environmental conditions, the cell temperature can vary. In particular, in the ANSYS model the cell temperature has been varied between 75°C and 105°C and it has been observed that the fluid temperature can reach values of about 90°C (Figure 15); so, a CPV/T system could be used for air heating and cooling applications. Referring to these assumptions, a CPV/T system with three modules of sixty cells each has been considered in the analysis and two different set-points have been fixed; in particular, 80°C in summer for the working of an absorber heat pump and 50°C in winter to obtain the sanitary hot water. The simulation reported in Figure 16 shows the space crossed by the fluid in the circuit. In particular, imposing the fluid velocity of 0.38 m/s and considering the length of each module equal to 17.6 m, about 47 rounds are necessary to reach the set-point of 50°C in winter, while 61 rounds are necessary in summer to obtain 80°C.

5. Conclusions

The experimental and theoretical analysis has allowed to evaluate the electrical parameters of the CPV system presented in this paper, the concentration factor, the cell temperature in different working conditions and the fluid temperature. In particular, the experimental values of the cell temperature have represented the input of the model, developed in ANSYS-CFX, able to evaluate the fluid temperature in the cooling circuit, realized with the CATIA software. Hence, both electrical and thermal aspects have been analyzed in order to evaluate the potential energy production of a CPV/T system. The experimental tests have been conducted at University of Salerno. First of all, an experimental analysis has been realized to define the best configuration of the CPV system modifying the optics. Fixing the solar direct irradiance, the I_{SC} and V_{OC} values have been obtained together with the maximum power point corresponding to the defined concentration. Moreover, the electric power and efficiency values and the cell temperature have been evaluated in different meteorological conditions: season, direct irradiance intensity and cloudiness. The experimental value of C has been about 208.6; this value has been used in the theoretical comparison in terms of electric power and efficiency. The experimental and theoretical electric powers have been compared in different working conditions. The cell efficiency for a sunny and a cloudy day has been also evaluated together with the related values of solar irradiance. Moreover, the fluid temperature trend has been evaluated considering the cell temperatures values reached in different operating conditions. The fluid temperature has been obtained by means of ANSYS-CFX and, considering higher concentrating factors and variable environmental conditions, the cell temperature can vary. Referring, for example, to an average cell temperature of 63°C in a summer day, the fluid has reached a temperature of about 55°C in four hours. Changing the cell temperature between 75°C and 105°C, a fluid temperature of about 90°C can be reached in a CPV/T system for air heating and cooling applications. Moreover, a CPV/T system with three modules of sixty cells each has been considered in the theoretical analysis. Fixing a fluid velocity of 0.38 m/s and considering the module length of 17.6 m, about 47 rounds have been necessary to reach the set-point of 50°C in winter, and 61 rounds in summer to obtain 80°C. Finally, the study presented of the electrical and thermal responses is a key-factor to realize a more complex prototype of a CPV/T system.

Nomenclature

A	area (m^2)
C	concentration factor
CFD	Computational Fluid Dynamics
CPC	compound parabolic concentrator
CPV	concentrating photovoltaic
CPV/T	concentrating photovoltaic and thermal
c	specific heat (kJ/kgK)
d	diameter (m)
FF	factor
G	Irradiance (W/m^2)
h	unitary convective conductance (W/m^2K)
I	current (A)
InGaP/InGaAs/Ge	indium-gallium-phosphide/indium- gallium-arsenide/germanium
K	conductance
m	mass (kg)
$\dot{m}$	mass flow rate (kg/s)
MJ	multi-junction
N	number
P	electric power (W)
T	temperature (°C)
x	space (m)
V	voltage (V)

Greek symbol

α	absorptivity coefficient
η	efficiency
θ	time (s)
σ_t	temperature coefficient (%/°C)

Subscripts

a	air
c	cell
dir	direct
f	fluid
i	indoor
inc	incident
int	intermediate
Kal	Kaleidoscope
mod	module
MPP	maximum power point
o	outdoor
oc	open circuit
opt	optic
ref	reference
SC	short-circuit
t	tube
tot	total
th	theoretical

References

[1] O. Z. Sharaf, M. F. Orhan, Concentrated photovoltaic thermal (CPVT) solar collector systems: Part I – Fundamentals, design considerations and current technologies, Renewable and Sustainable Energy Reviews 60 (2016) 1500–1565.

[2] Z. Xu, C. Kleinstreuer, Concentration photovoltaic–thermal energy co-generation system using nanofluids for cooling and heating, Energy Conversion and Management 87 (2014) 504-512.

[3] O. Z. Sharaf, M. F. Orhan, Concentrated photovoltaic thermal (CPVT) solar collector systems: Part II – Implemented systems, performance assessment and future directions, Renewable and Sustainable Energy Reviews 50 (2015) 1566–1633.

[4] S.Jakhar, M.S. Soni, N.Gakkhar. Historical and recent development of concentrating photovoltaic cooling technologies. Renewable and Sustainable Energy Reviews 60 (2016) 41–59.

[5] M. Li, G.L. Li, X. Ji, F. Yin, L. Xua, The performance analysis of the trough concentrating solar photovoltaic/thermal system, Energy Conversion and Management 52 (2011) 2378-2383.

[6] C. Kandilli, Performance analysis of a novel concentrating photovoltaic combined system, Energy Conversion and Management 67 (2013) 186-196.

[7] F. Chaoqing, Z. Hongfei, W. Rui, M. Xinglong, Performance investigation of a concentrating photovoltaic/thermal system with transmissive Fresnel solar concentrator, Energy Conversion and Management 111 (2016) 401–408.

[8] K. Yang, C. Zuo, A novel multi-layer manifold microchannel cooling system for concentrating photovoltaic cells, Energy Conversion and Management 89 (2015) 214-221.

[9] I.Ceylan, A.E.Gu¨rel, A.Ergu¨n, A.Tabak. Performance analysis of a concentrated photovoltaic and thermal system, Solar Energy 129 (2016) 217–223.

[10] X.Meng,N.Sellami, A.R.Knox, A.Montecucco, J.Siviter, P.Mullen, A.Ashraf, A.Samarelli, L.F. Llin, D.J.Paul, W.Li, M.C.Paul, D.H.Gregory, G.Han, M.Gao, T.Sweet, R.Freer, F.Azough, R.Lowndes,X.Xia,T.K.Mallick. A novel absorptive/reflective solar concentrator for heat and electricity generation: An optical and thermal analysis, Energy Conversion and Management 114 (2016) 142–153.

[11] C. Renno, F. Petito, Design and modeling of a concentrating photovoltaic thermal (CPV/T) system for a domestic application, Energy and Buildings 62 (2013) 392-402.

[12] C. Renno, Optimization of a concentrating photovoltaic thermal (CPV/T) system used for a domestic application, Applied Thermal Engineering 67 (2014) 396-408.

[13] C. Renno F. Petito, Choice model for a modular configuration of a point-focus CPV/T system, Energy and Buildings 92 (2015) 55-66.

[14] M. Imtiaz Hussain, G.H. Lee, Experimental and numerical studies of a U-shaped solar energy collector to track the maximum CPV/T system output by varying the flow rate, Renewable Energy 76 (2015) 735-742.

[15]F. Almonacid, E.F. Fernandez, T.K. Mallick, P.J. Perez-Higueras, High concentrator photovoltaic module simulation by neuronal networks using spectrally corrected direct normal irradiance and cell temperature, Energy 84 (2015) 336-343.

[16] T. Kerzman, L. Schaefer, System simulation of a linear concentrating photovoltaic system with an active cooling system, Renewable Energy 41 (2012) 254–61.

[17] C. Renno, M. De Giacomo, Dynamic simulation of a CPV/T system using the finite element method, Energies 7 (2014) 7395-7414.

[18] S.K.Natarajan, M.Katz, R.Ebner, S.Weingaertner, O.Aßländer, A.Cole, R.Wertz, T.Giesen, T.K. Mallick. Experimental validation of a heat transfer model for concentrating photovoltaic system, Applied Thermal Engineering 33-34 (2012) 175-182.

[19] P.Rodrigo, E.F.Fernández, F.Almonacid, P.J.Pérez-Higueras, Review of methods for the calculation of cell temperature in high concentration photovoltaic modules for

electrical characterization, Renewable and Sustainable Energy Reviews 38 (2014) 478–488.

[20] G. Calabrese, F. Gualdi, S. Baricordi, P. Bernardoni, V. Guidi , L. Pozzetti , D. Vincenz, Numerical simulation of the temperature distortions in InGaP/GaAs/Ge solar cells working under high concentrating conditions due to voids presence in the solder joint, Solar Energy 103 (2014) 1–11.

[21] A. B. Or, J. Appelbaum, Dependence of multi-junction solar cells parameters on concentration and temperature, Solar Energy Materials & Solar Cells, 130 (2014) 234–240.

[22] ANSYS ® Academic Research, release 16.2, Help System, ANSYS Inc.

[23] C. Renno, F. Petito, A. Gatto. Artificial neural network models for predicting the solar radiation as input of a concentrating photovoltaic system, Energy Conversion and Management 106 (2015) 999–1012.

[24] D. Chemisana, A. Vossier, L. Pujol, A. Perona, A. Dollet. Characterization of Fresnel lens optical performances using an opal diffuser, Energy Conversion and Management 52 (2011) 658–663.

[25] Triple-Junction Solar Cell for Terrestrial Applications. CTJ photovoltaic cell –5.5 mm x 5.5 mm, Datasheets Emcore September 2012. Emcore Corporation.

[26] R.Mastrullo, C.Renno. A thermoeconomic model of a photovoltaic heat pump, Applied Thermal Engineering 30 (2010) 1959-1966.

[27] C.Aprea and C.Renno. An experimental analysis of a thermodynamic model of a vapour compression refrigeration plant on varying the compressor speed. International Journal of Energy Research 28 (2004) 219-228.

[28] CATIA: Dassault Systèmes - http://www.3ds.com/products-services/catia

[29] G.Di Gironimo, C.Labate, F.Renno, G.Brolatti, F.Crescenzi, F.Crisanti, A.Lanzotti, F.Lucca, Concept Design of Divertor Remote Handling System for the FAST Machine, Fusion Engineering and Design, 88 (2013) 2052-2056.

[30] G.Ramogida, G.Calabrò, V.Cocilovo, F.Crescenzi, F.Crisanti, A.Cucchiaro, G. Di Gironimo, R.Fresa, V.Fusco, P.Martin, S.Mastrostefano, R.Mozzillo, F.Nuzzolese, F.Renno, C.Rita, F.Villone, G.Vlad. Active toroidal field ripple compensation and MHD feedback control coils in FAST, Fusion Engineering and Design 88 (2013) 1156-1160.

[31] C.Aprea and C.Renno. A numerical approach to a very fast thermal transient in an air cooling evaporator. Applied Thermal Engineering 22 (2002) 219-228.

[32] A. Akisawa, M. Hiramatsu, K. Ozaki, Design of dome-shaped non-imaging Fresnel lenses taking chromatic aberration into account, Solar Energy 86 (2012) 877–885.

[33] C.Aprea and C. Renno. Experimental model of a variable capacity compressor. International Journal of Energy Research 33 (2009) 29-37.

[34] C.Aprea and C.Renno. An air cooled tube-fin evaporator model for an expansion valve control law. Math. Comput. Model. 30 (1999) 135-146.

[35] W. Zilong, Z. Hua, W. Dongsheng, Z. Wei, Z. Zhigang, Characterization of the InGaP/InGaAs/Ge triple-junction solar cell with a two-stage dish-style concentration system, Energy Conversion and Management 76 (2013) 177–184.

Tables captions

Table 1 Triple-junction cell characteristics

Table 2 Thermal resistances values

Figures captions

Figure 1 CPV system photo

Figure 2 CPV system scheme

Figure 3 Flow-chart of the experimental-theoretical analysis

Figure 4a Scheme of the parts involved in the heat transfer

Figure 4b Thermal resistances scheme related to the insulated and not insulated walls

Figure 5 Geometric model of the cooling circuit realized by means of CATIA

Figure 6 Definition of the domains in ANSYS

Figure 7 Concentration factor of the experimental plant

Figure 8 Experimental and theoretical comparison of the electric power (summer day)

Figure 9 Experimental and theoretical comparison of the electric power (winter day)

Figure 10 Electric efficiency as function of the solar irradiance

Figure 11Experimental values of the cell temperature in different months

Figure 12 Fluid temperature as function of the experimental cell temperature (summer day)

Figure 13 Fluid temperature as function of the experimental cell temperature (winter day)

Figure 14 Fluid temperature trend determined in ANSYS

Figure 15 Theoretical fluid temperature varying the working conditions

Figure 16 Fluid temperature along the circuit

Table(s)

Table 1 Triple-junction cell characteristics

Triple junction cell	
Parameter	***Value***
material	InGaP/InGaAs/Ge
dimensions	5.5 mm x 5.5 mm
η_r (at 25 °C, 50 W/cm^2 - 1000 suns)	39.0%
temperature coefficient (σ_t)	-0.04%/°C

Table(s)

Table 2 Thermal resistances values

	Thickness [m]	***Conductivity [W/mk]***	***Thermal resistance [m^2 K/W]***
Solar cell	1.00 E-03	148	6.76 E-06
Copper	3.00 E-03	390	7.70 E-06
Epoxy resin	1.00 E-4	1.38	7.25 E-05
Insulator	5.00 E-3	0.014	0.36 E+00

Figure(s)

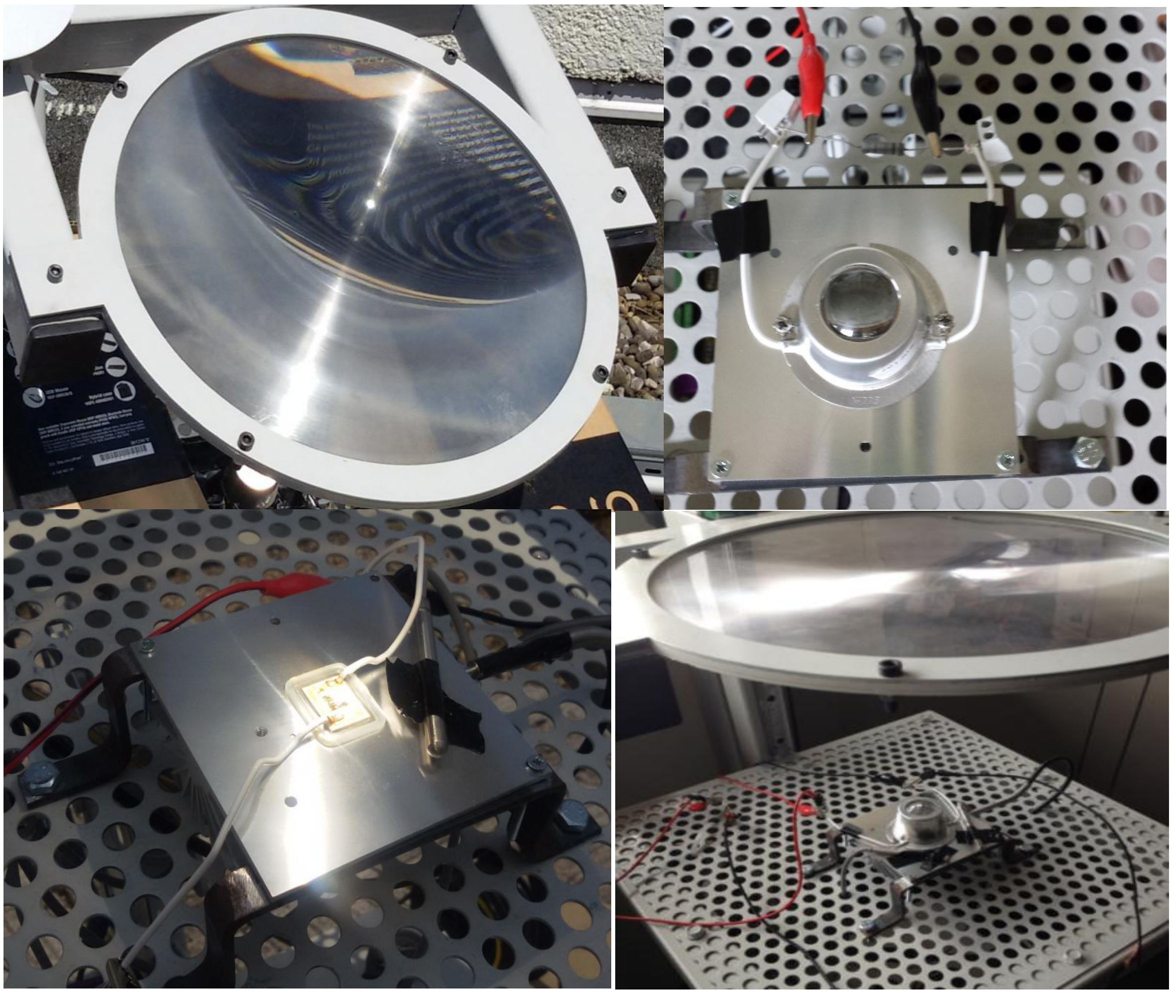

Figure 1 CPV system photo

Figure(s)

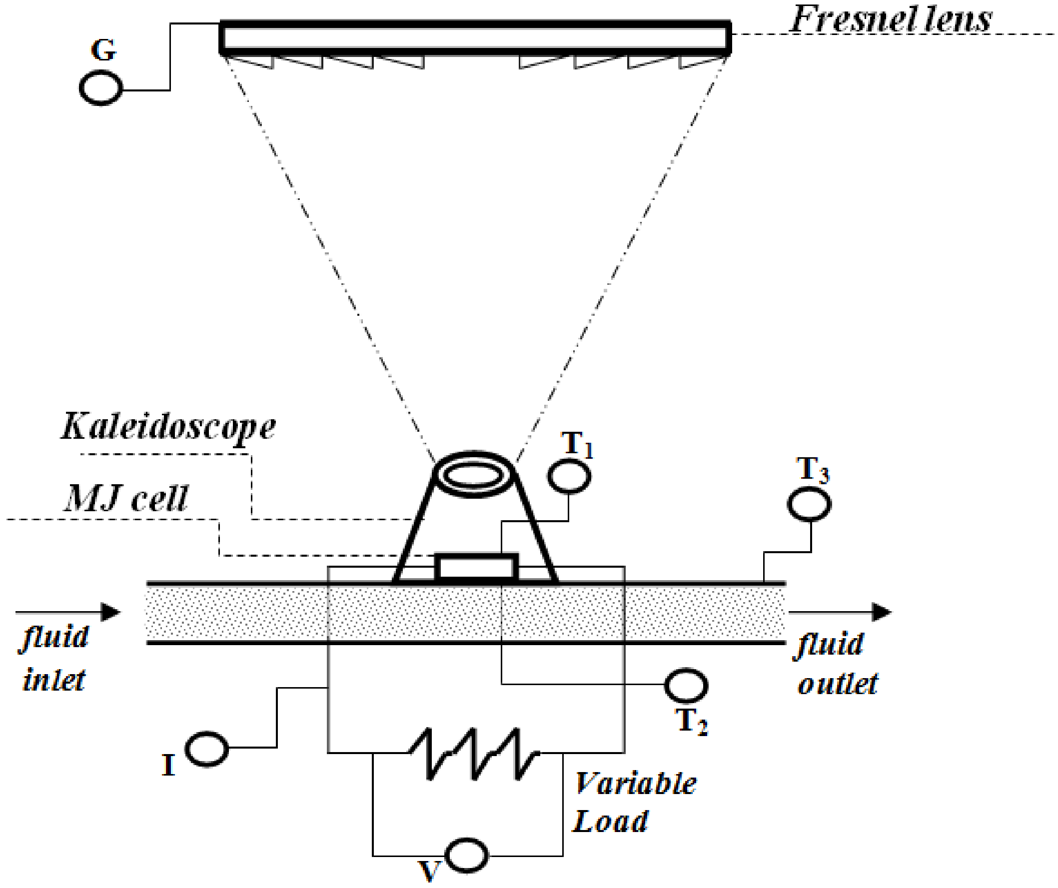

Figure 2 CPV system scheme

Figure(s)

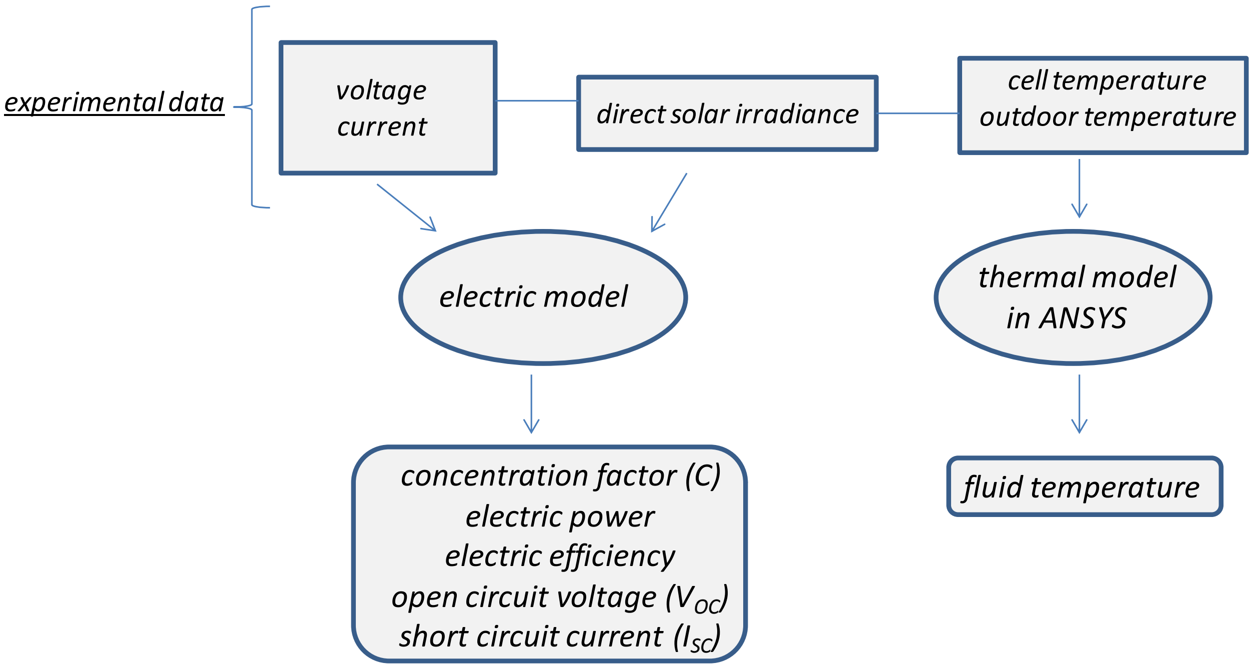

Figure 3 Flow-chart of the experimental-theoretical analysis

Figure(s)

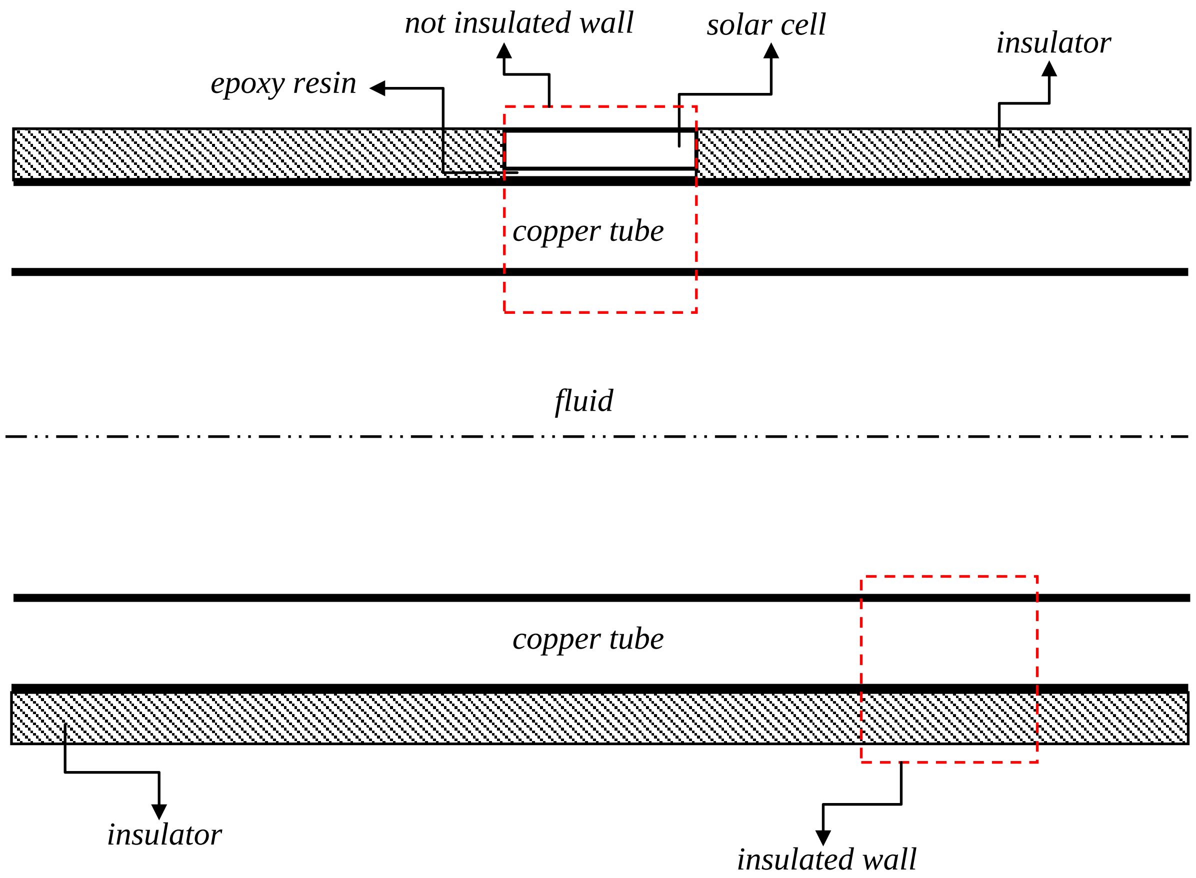

Figure 4a Scheme of the parts involved in the heat transfer

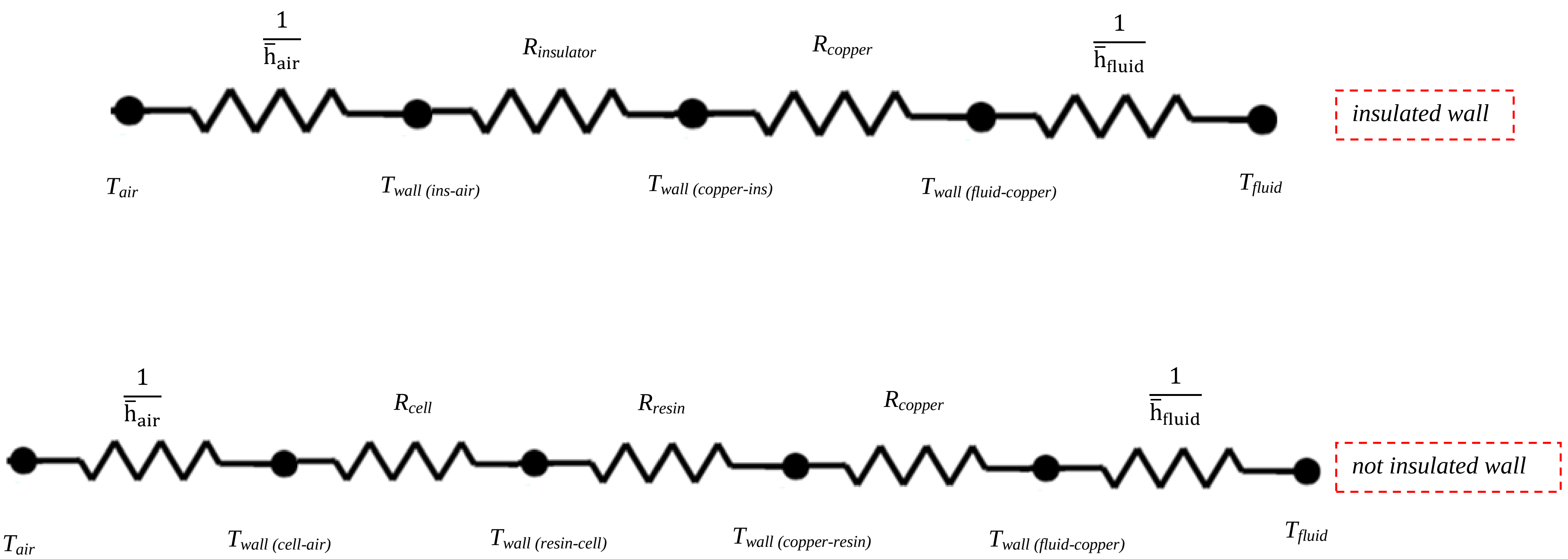

Figure 4b Thermal resistances scheme related to the insulated and not insulated walls

Figure(s)

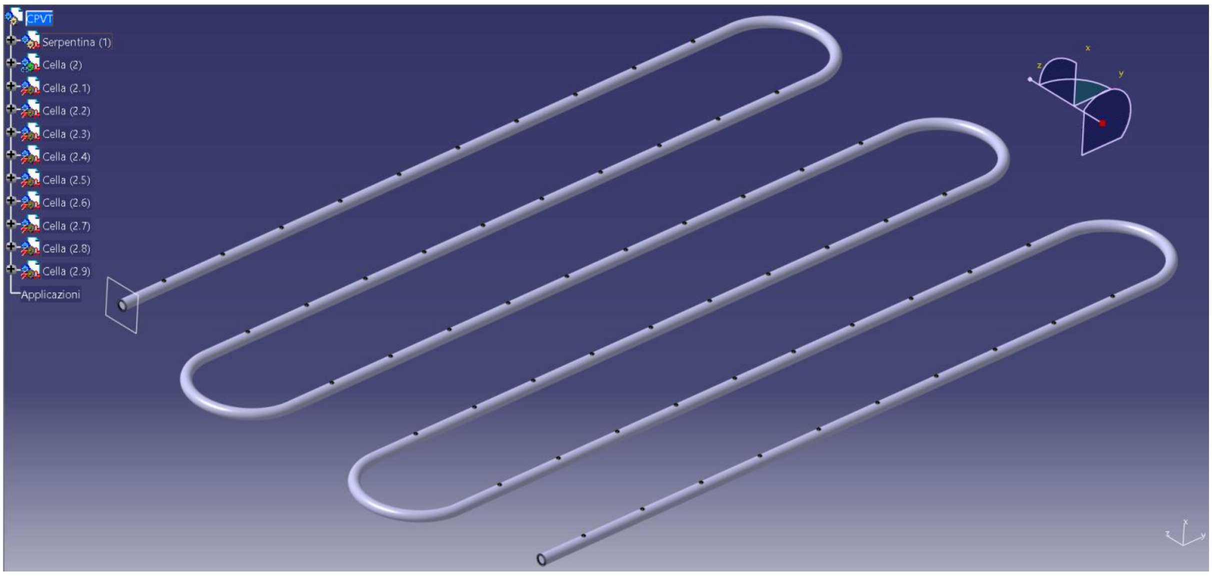

Figure 5 Geometric model of the cooling circuit realized by means of CATIA

Figure(s)

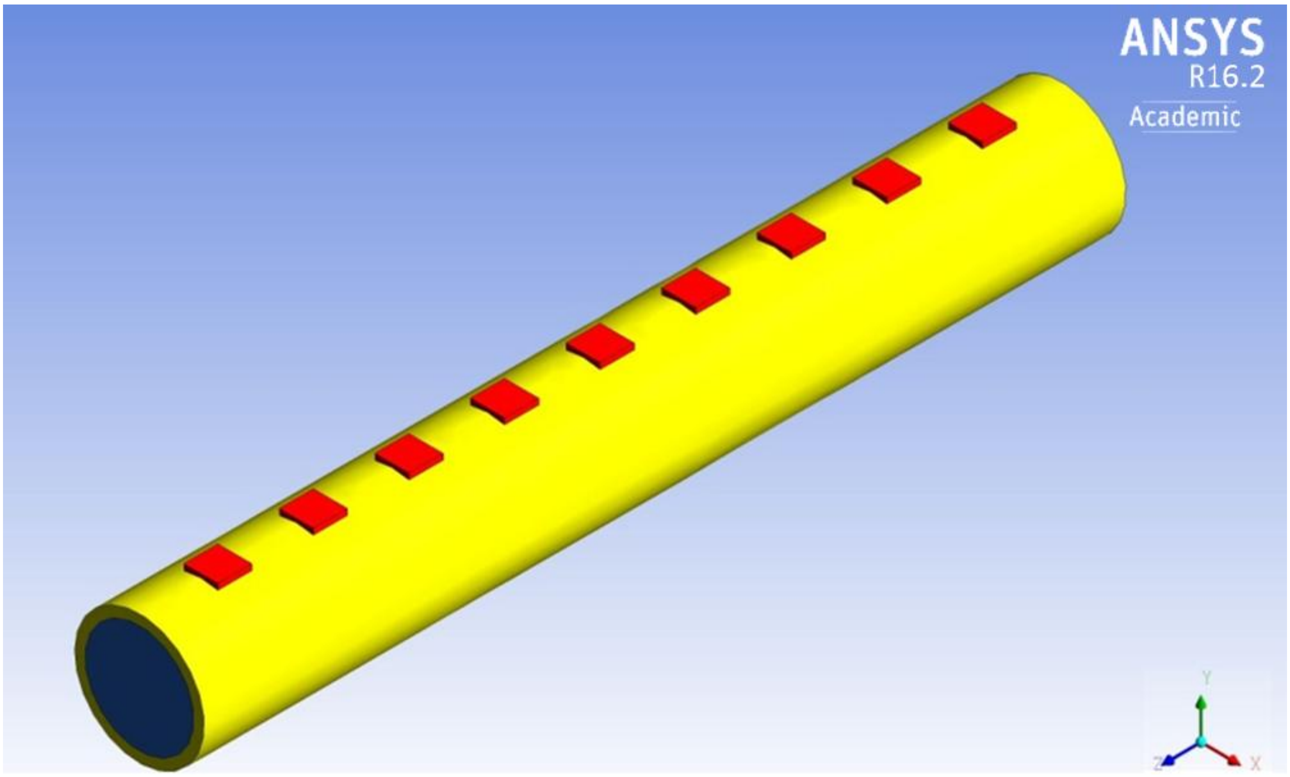

Figure 6 Definition of the domains in ANSYS

Figure(s)

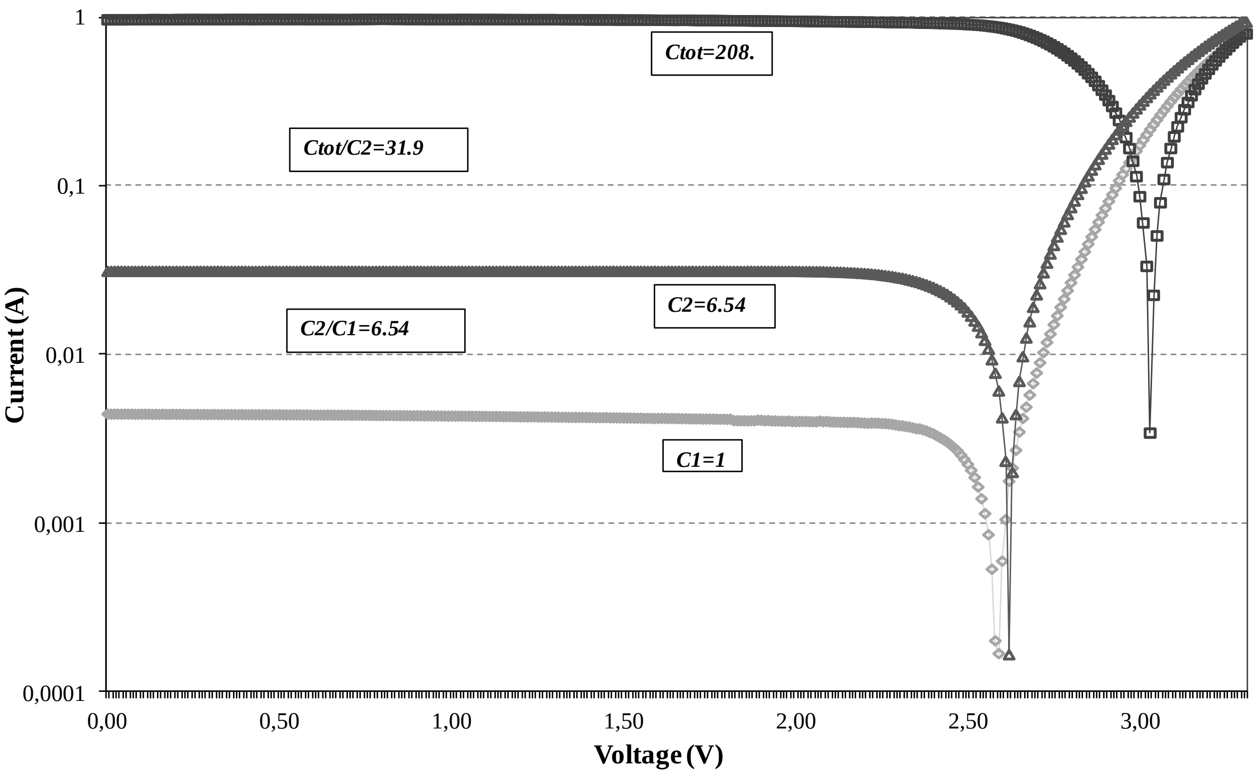

Figure 7 Concentration factor of the experimental plant

Figure(s)

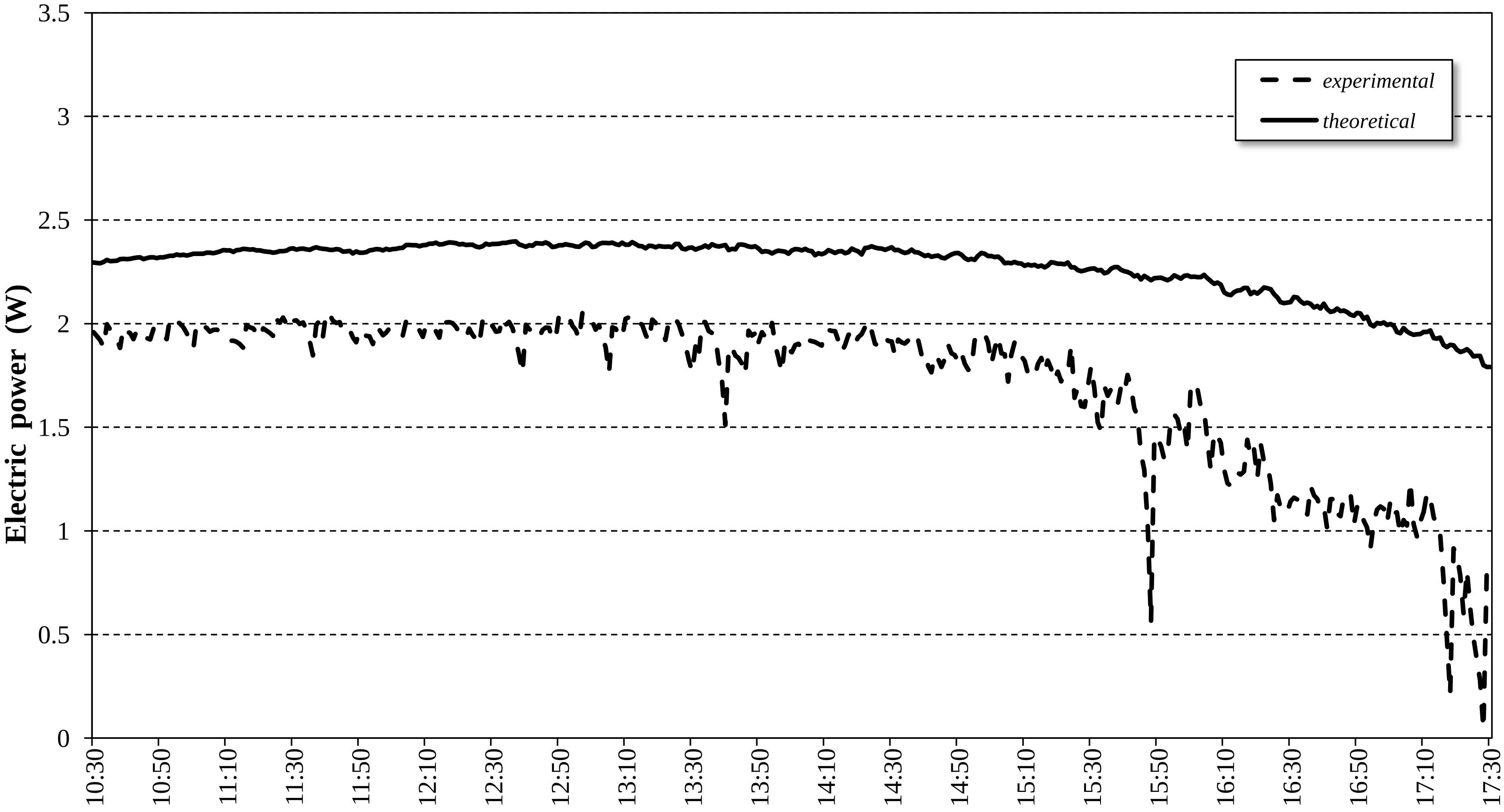

Figure 8 Experimental and theoretical comparison of the electric power (summer day)

Figure(s)

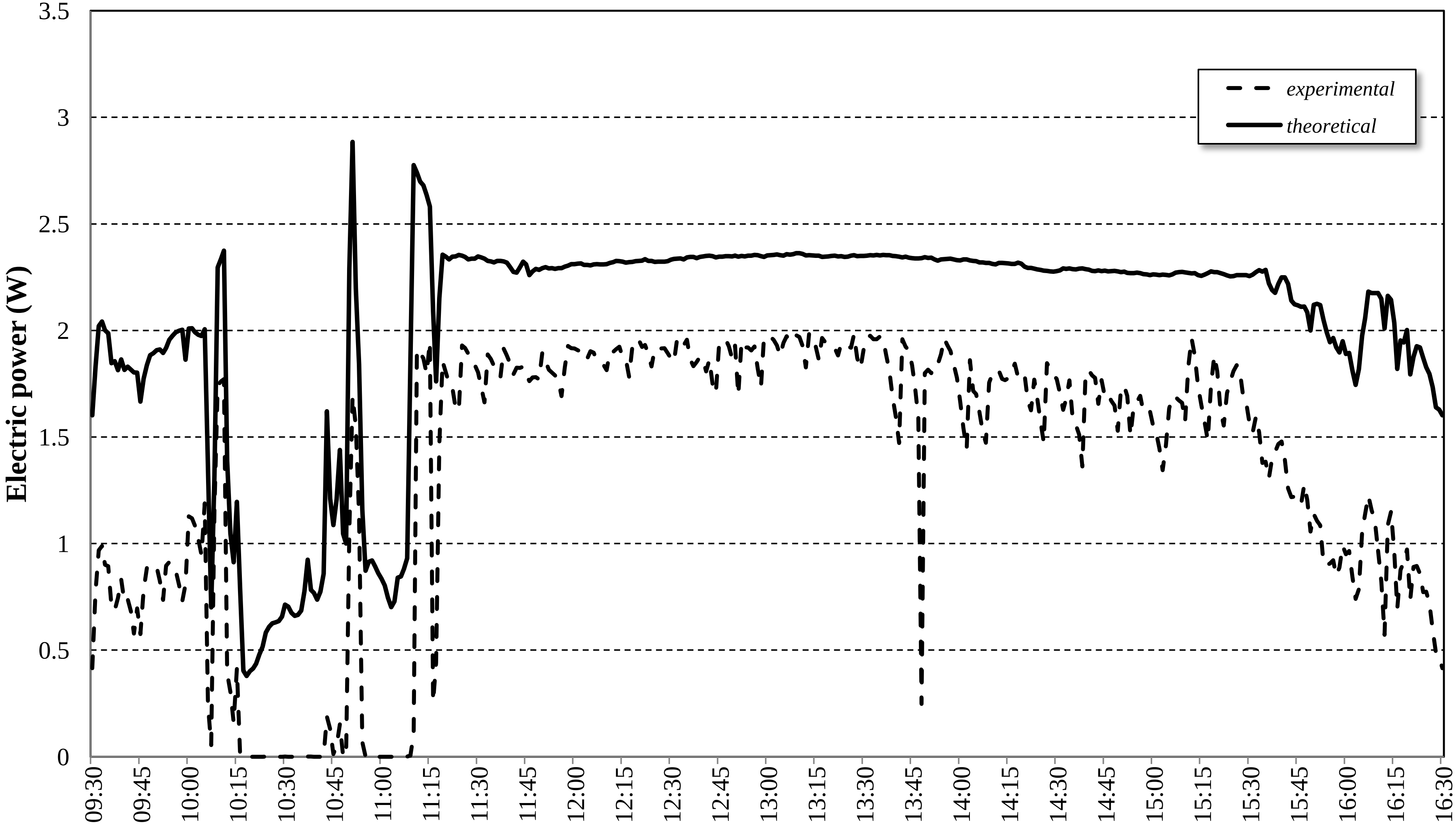

Figure 9 Experimental and theoretical comparison of the electric power (winter day)

Figure(s)

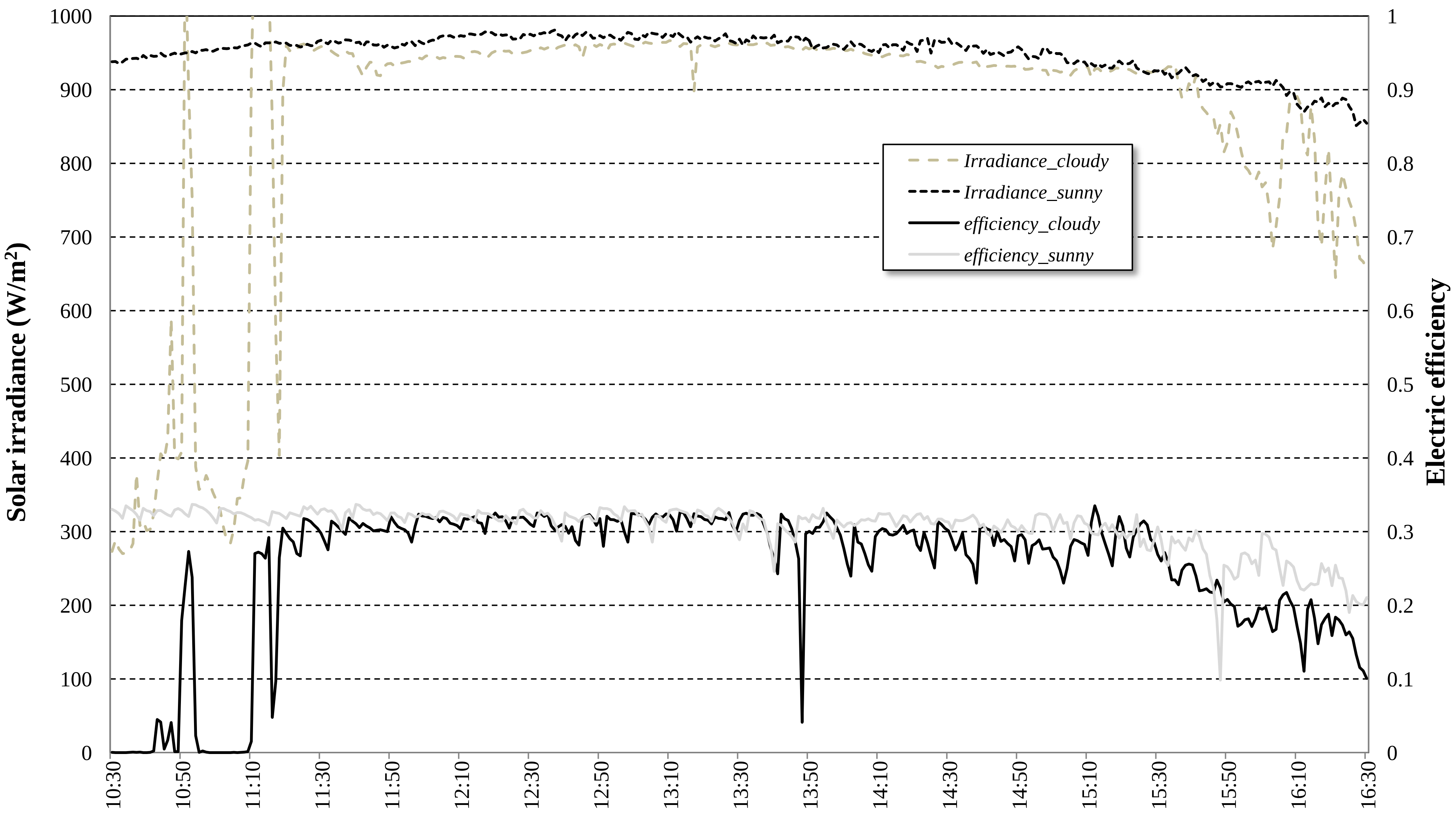

Figure 10 Electric efficiency as function of the solar irradiance

Figure(s)

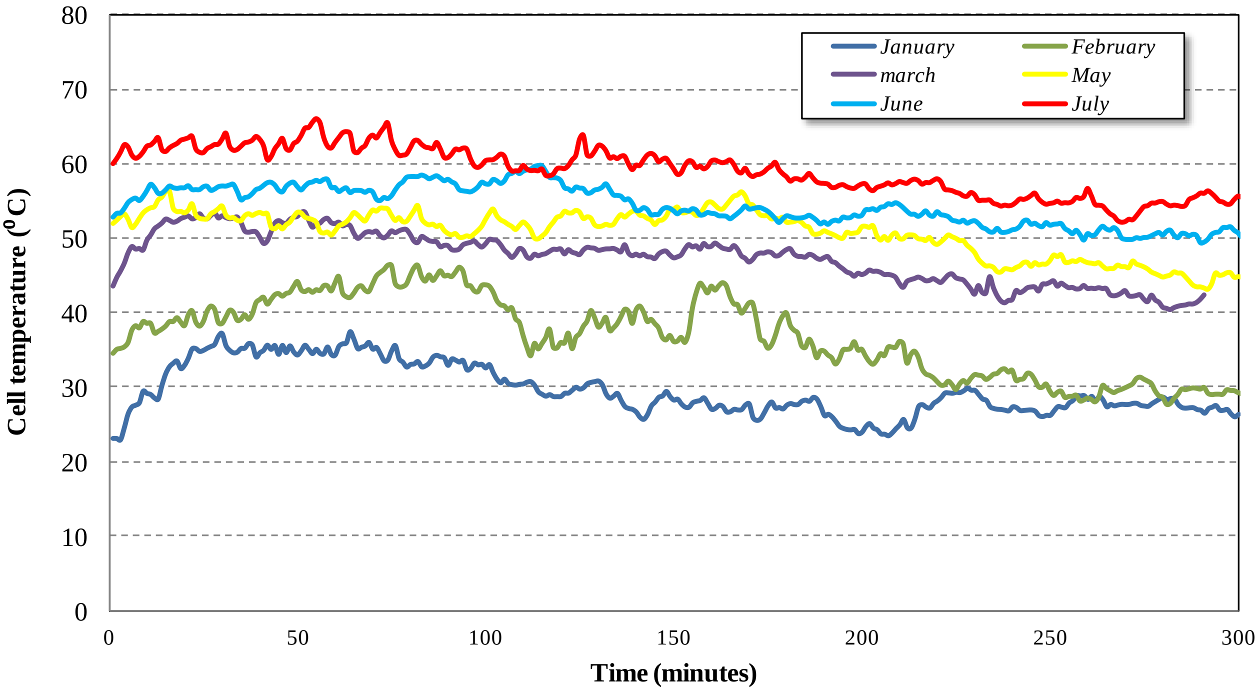

Figure 11Experimental values of the cell temperature in different months

Figure(s)

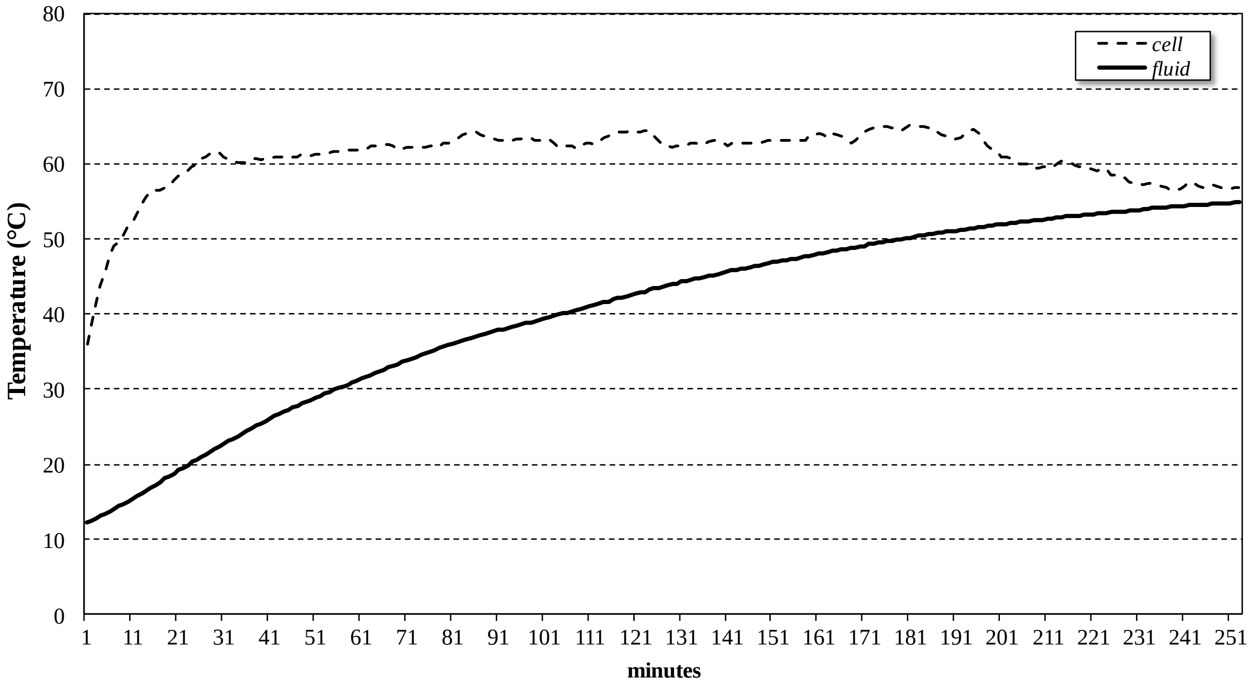

Figure 12 Fluid temperature as function of the experimental cell temperature (summer day)

Figure(s)

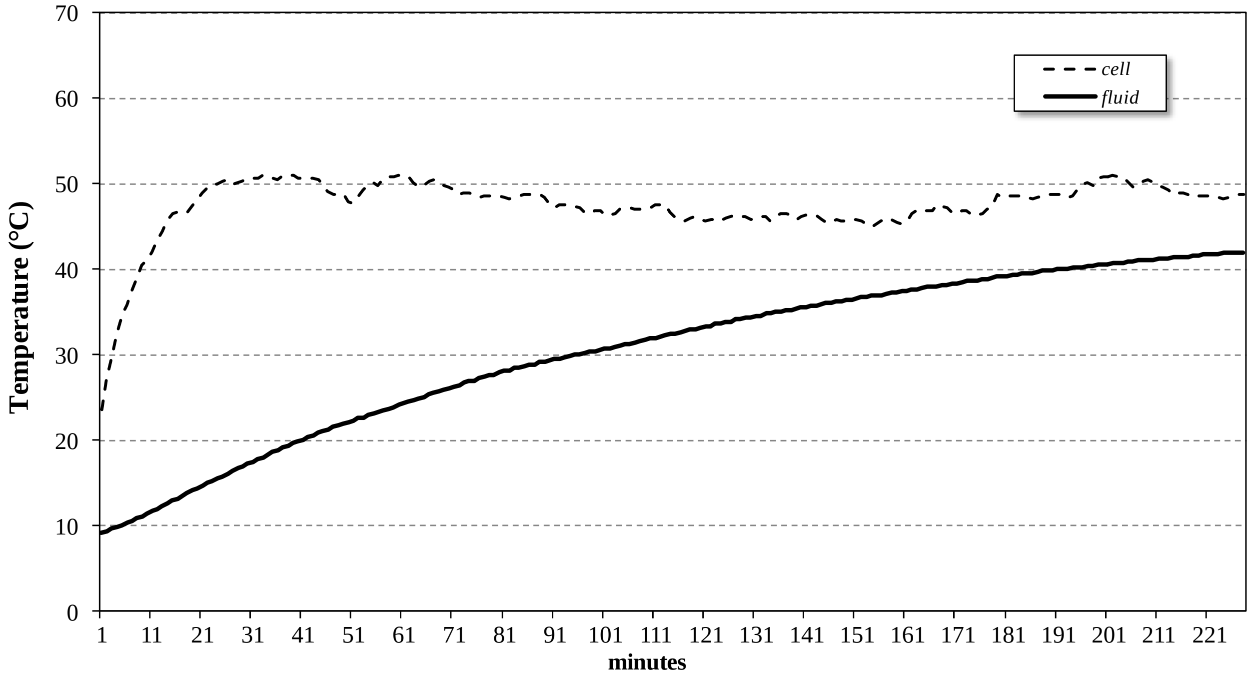

Figure 13 Fluid temperature as function of the experimental cell temperature (winter day)

Figure(s)

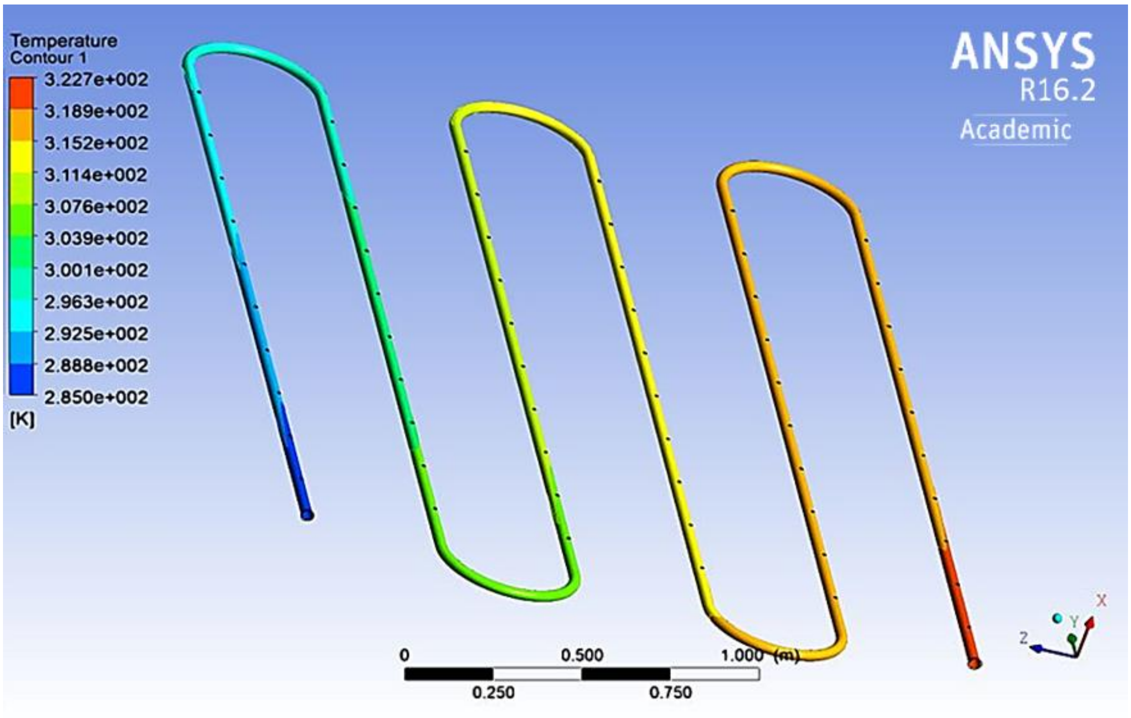

Figure 14 Fluid temperature trend determined in ANSYS

Figure(s)

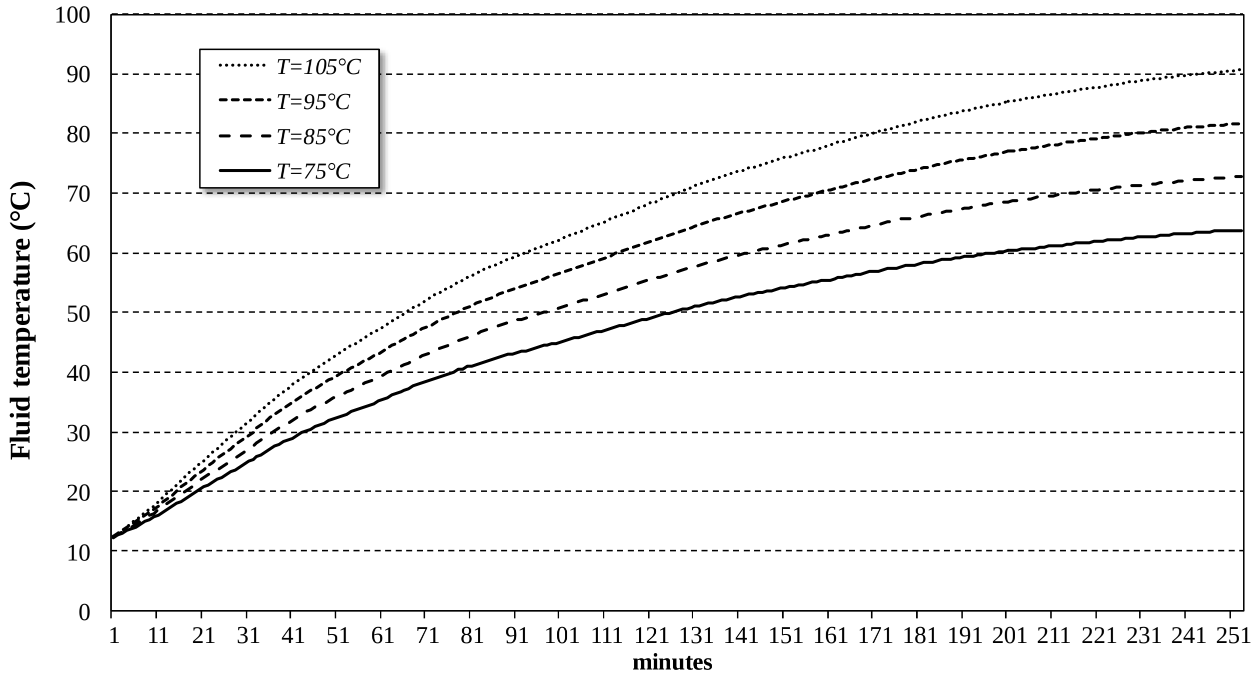

Figure 15 Theoretical fluid temperature varying the working conditions

Figure(s)

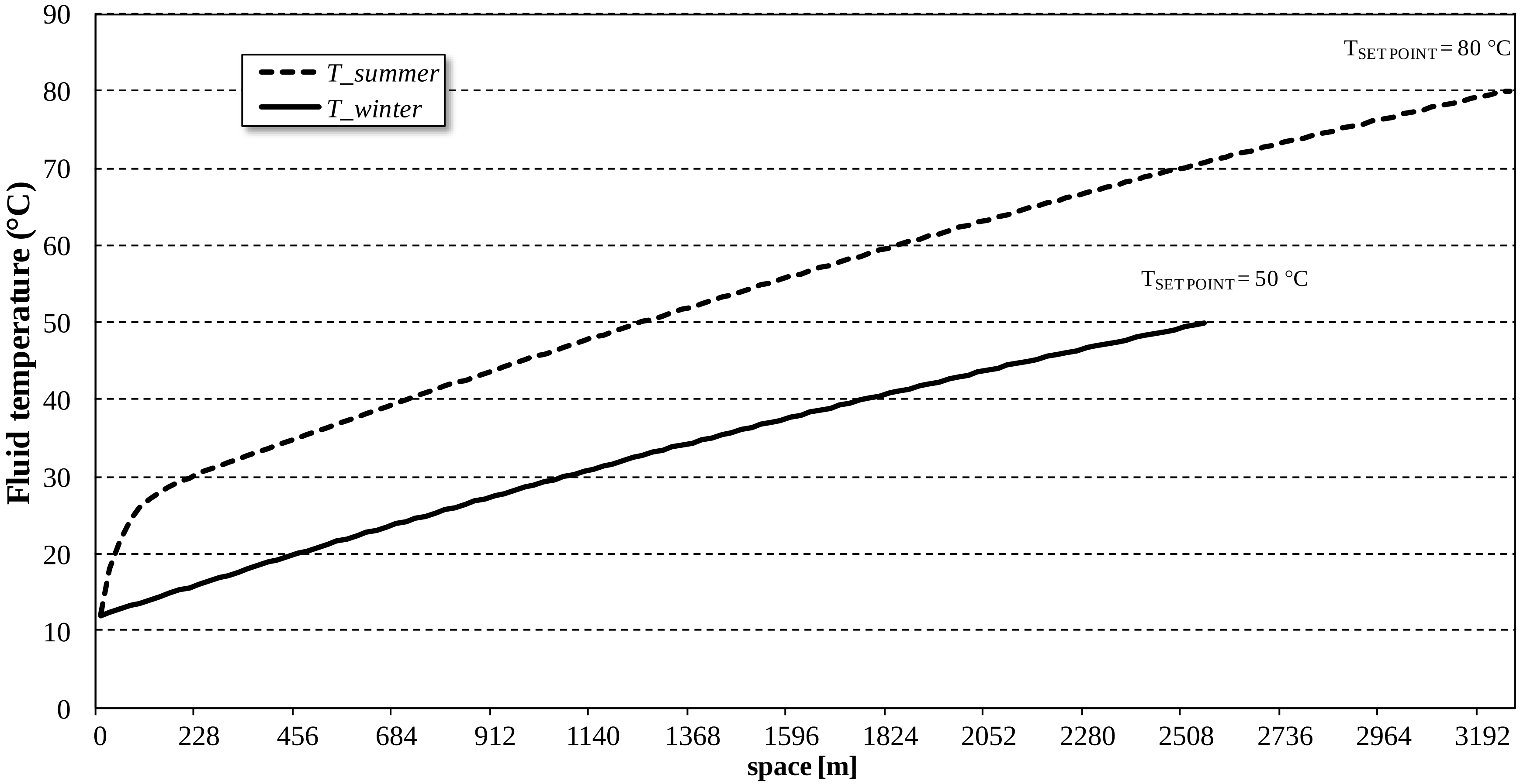

Figure 16 Fluid temperature along the circuit